BIOMECHANICAL EFFECTS OF A ROBOTIC KNEE EXOSKELETON DURING SLOPE WALKING

A Dissertation
Presented to
The Academic Faculty

by

Dawit Lee

In Partial Fulfillment
of the Requirements for the Degree
Master of Science in the
School of Mechanical Engineering

Georgia Institute of Technology
December 2018

BIOMECHANICAL EFFECTS OF A ROBOTIC KNEE EXOSKELETON DURING SLOPE WALKING

Approved by:

Dr. Aaron J. Young, Advisor
School of Mechanical Engineering
Georgia Institute of Technology

Dr. Gregory Sawicki
School of Mechanical Engineering
Georgia Institute of Technology

Dr. Young-Hui Chang
School of Biological Sciences
Georgia Institute of Technology

Date Approved: [11 16, 2018]

ACKNOWLEDGEMENTS

I would have not been able to present this work here without the people named here. First of all, I would like to thank Dr. Aaron Young for his tremendous support and grateful advice for this research work. I would like to express my gratitude to Inseung Kang for his help and mentorship from the first day in the lab to the end of this work.

I would like to especially acknowledge my friend and colleague Eun Chan Kwak. I deeply appreciate for the commitment and sacrifice you have shown for making this work happen for the past two years.

I would like to thank rest of the outstanding undergraduate students that I had chances to work with: Bailey McLain, Chris Mao, Michelle Myrick, Morgan Childress, and George Niu. I would like to thank rest of the members of the EPIC lab for sharing ideas and supporting each other.

I would like to thank Dr. Geza Kogler for providing consultation opportunities for orthotic interfaces. I would also like to thank and acknowledge Dr. Greg Sawicki and Dr. Young-Hui Chang for serving as committee members for my thesis.

I would like to thank Kyle French and Andrew Keller at the Mechanical Engineering Electronics Lab for their assistance in circuit design. I would like to also thank all the members of the Montgomery Machining Mall for helping me with machining.

Last but not least, my parents and brother. I love you, and thank you for supporting me throughout my life.

TABLE OF CONTENTS

LIST OF TABLES

LIST OF FIGURES

LIST OF SYMBOLS AND ABBREVIATIONS

AL	Assisted leg
UAL	Unassisted leg
BF	Biceps femoris
GA	Gastrocnemius
ST	Semitendinosus
VL	Vastus lateralis
VM	Vastus medialis
RF	Rectus femoris

SUMMARY

Powered exoskeleton is a promising wearable robotic technology that holds a large area of potential implementations including human augmentation, mobility assistance, and rehabilitation. One of the major goals in the field of exoskeleton research has been to reduce the human's energetic consumption by partially replacing the biological muscle work required to perform certain tasks. A majority of these exoskeletons are targeting either the ankle or the hip joint due to their large contribution in providing positive mechanical work. While these joint contributions may overshadow the knee joint in level-ground walking, its role becomes greater in the case of sloped walking. Additionally, the research in investigating the biomechanical effectiveness of knee exoskeleton has been generally sparse. Consequently, it is sought to investigate the efficacy of the use of a knee exoskeleton in slope walking where the role of the knee joint becomes more important in terms of power output/absorption.

In this thesis, a study in the biomechanical effectiveness of the use of a robotic unilateral knee exoskeleton during incline and decline walking on healthy adults is presented. The first hypothesis of the study is that the extension torque assistance during the early stance phase would reduce the muscle activation reduction of the knee extensors on the assisted leg that are normally responsible of the assisted motion. The second hypothesis is that the reduction in the knee extensor muscle activation of the assisted leg would reduce the metabolic cost.

A human-subject experiment was performed, and the result from the experiment shows that the knee extensor group of the assisted leg significantly reduced their activation

with assistance in both incline and decline walking. However, there are a group of individuals who reduce their metabolic cost with the assistance using the knee exoskeleton and a group of individuals did not. The main biomechanical causes of the increase in metabolic cost in incline walking with assistance seems to be the increase in knee extensors' muscle activity on the unassisted leg and the increase in total positive power generation in both legs combined. The main biomechanical cause of the increase in metabolic cost in decline walking with assistance seems to be the nonresponder's assisted leg was heavily relying on the ankle joint for the majority of the power absorption. For the use of a unilateral knee exoskeleton, the interaction between legs as well as the interaction between the device and the user should be heavily consider to produce energetic benefit from the exoskeleton.

CHAPTER 1. INTRODUCTION

Over the past years, both research and industry fields have actively focused on developing powered lower-limb exoskeletons. These devices can mainly be categorized into three major applications: human performance augmentation, mobility assistance, and rehabilitation [1]. Human performance augmentation utilizes these exoskeleton devices to reduce the workload from the users working in an industrial or factory setting as well as soldiers walking long distances with carrying heavy loads [1-3]. Moreover, powered exoskeletons can also be employed to provide partial assistance to healthy individuals. This assistance can be applied into different locomotion modes such as walking, stair ascent/descent, and ramp ascent/descent [4-6]. Lastly, exoskeletons are used in therapeutic and rehabilitative purposes for patients with gait deficiencies [7, 8]. One of the major goals in the field of exoskeleton research has been to reduce the human's energetic consumption by partially replacing the biological muscle work required to perform certain tasks [1]. In the case of walking (i.e. level-ground), which is often the primary focus, the majority of these exoskeletons have targeted either the ankle or the hip joint due to their core contribution in providing positive mechanical work [9]. The knee joint creates the smallest portion of the total positive mechanical work among the lower-limb joints in level-ground walking [9], making it the least common lower limb joint to augment for locomotion assistance. While these joint contributions may overshadow the knee joint in level-ground walking, its role becomes greater in the case of sloped walking. For instance, walking incline is highlighted by a significant amount of positive power generation needed to carry the center of mass (COM) of the body forward and up while fighting against the gravity.

As the locomotion mode translates from level-ground to incline, the percent contribution of the knee joint to the total positive work of the leg over the stance phase significantly increases while the percent contribution of the ankle to the total positive work of the leg over the stance phase decreases [10] as shown on the top row in Figure 1.1.

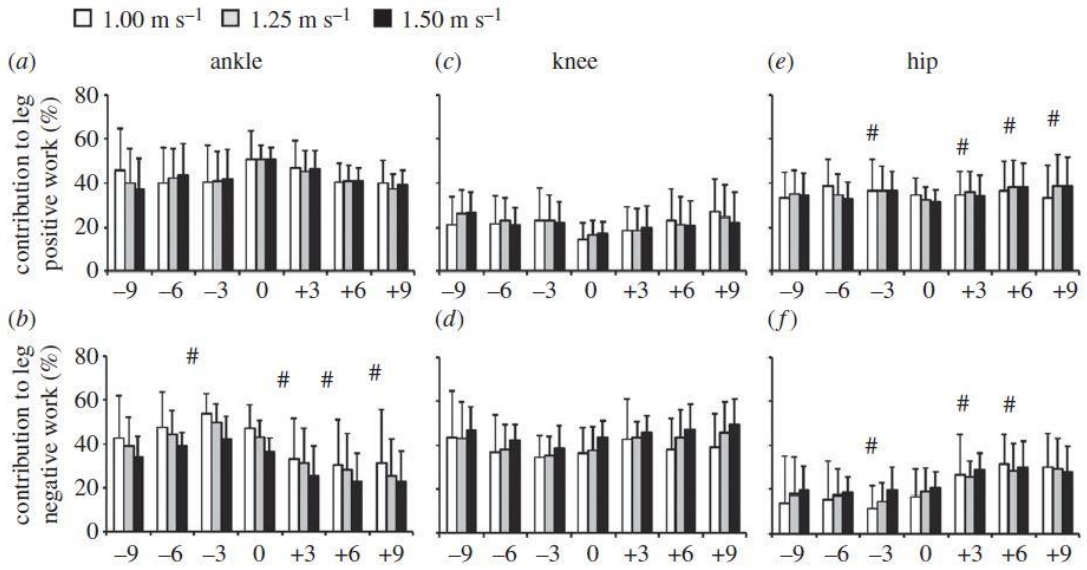

Figure 1.1: Average (standard deviation) percent contribution of the ankle (a,b), knee (c,d), and hip (e,f) to total positive and negative individual leg work over the stance phase at 1.00 (white), 1.25 (grey), and 1.50 (black) m/s on slopes of -9° to +9° [10]

This trade-off trend between the ankle and the knee joint is also exhibited in terms of the percent negative work contribution over the stance phase between level-ground and decline walking [10] as shown on the bottom row in Figure 1.1. These increases in the demanded knee joint work effort is reflected by the increase in the knee extension moment in both incline and decline walking compared to level-ground walking. During incline walking, the peak knee extension moment during stance phase increases by more than five times

compared to level-ground walking [11]. During decline walking, the knee mainly functions as a shock-absorber by creating a substantial amount of negative work during the weight-acceptance phase [12]. The knee produces a significant amount of extension moment to prevent collapse of the body, and the peak moment is about two times that of the peak extension moment the knee produces during level-ground walking [12]. This increase in the knee extension moment generation is directly linked to a substantial increase in the knee extensors activation [13]. This activation eventually leads to an elevation of the patellofemoral compression force, which is more than four times during both walking incline and decline compare to level-group walking [14]. Therefore, assisting the knee using an exoskeleton offers the potential capability to assist in tasks that are often much more difficult and energetically demanding versus level-walking and also reduce potential risks in damaging the knee joint from increased muscle activity.

There are a number of previous research studies involved in developing and investigating the efficacy of knee exoskeleton use for human augmentation. Figure 1.2 highlights specific examples of previous knee exoskeleton research works. First, there were many previous research works focusing on the mechanical design and controls aspects. A few research works focused on developing mechanical designs that are adaptive to the positional change of the knee joint center that exhibit polycentricity [15-18]. *Shepherd et al.* developed a torque-controllable knee exoskeleton using ball screw drive and series elastic actuator (SEA) for sit-to-stand assistance [4]. *Karavas et al.* also designed a knee exoskeleton, called CompAct-RS, with series elastic actuator (SEA) to be used for walking, sit-to-stand, or squatting movement [19]. This exoskeleton was tested with tele-impedance based controller [20]. *Zhu et al.* has developed a torque dense, highly back drivable,

powered knee-ankle exoskeleton using a belt-drive power transmission system for rehabilitation purpose [21]. *Shamaei et al.* designed and evaluated a quasi-passive knee-ankle-foot orthosis to assist the knee joint in stance phase during walking by adding controllable stiffness to the knee joint [22].

Figure 1.2: KNEXO (left) is a unilateral pneumatic knee exoskeleton for level-ground walking [23], torque-controllable knee exoskeleton for sit-to-stand assistance (middle) designed by *Shepherd et al.* [4], and a clutch-spring knee exoskeleton for running (right) by *Elliot et al* [24]

One research group has investigated the human-robot interaction by looking at spatio-temporal gait parameters, kinematics, and muscle activity of the users using a unilateral pneumatic knee exoskeleton [23]. *Elliot et al.* has investigated the biomechanical

and energetic effect of a clutch-spring knee exoskeleton that added an energy storage-return spring element to assist knee extension in stance phase [25]. In general, the list of the previous knee exoskeleton research works often lack a focus on the biomechanical aspect of the study and focuses more on hardware and control strategies. Additionally, to the author's knowledge, the energetic effect of using a powered knee exoskeleton has not been investigated in incline or decline walking modes.

Consequently, it is sought to investigate the efficacy of the use of a knee exoskeleton where the role of the knee joint becomes more important in terms of power output/absorption. In this thesis, a study in the biomechanical effectiveness of the use of a robotic unilateral knee exoskeleton during sloped walking on healthy adults is presented. The first hypothesis of the study was that the knee extension torque assistance during the early stance phase will reduce the knee extensor muscle activation of the assisted leg (AL). The second hypothesis was that the reduction in the knee extensor muscle activation of the AL would lead to a reduction in metabolic cost of the users. The hypotheses were based on the previous literature that have demonstrated metabolic cost reduction when a powered assistance was provided to partially replace the joint biological effort required [5, 26, 27].

CHAPTER 2. DEVICE

2.1 Design Objective

The powered knee exoskeleton was designed to partially replace a human's biological knee moment during different types of walking. The main aspects of the device specifications are presented in Table 1. The maximum speed of the actuator matches the level of maximum speed of the knee joint in level-ground walking which is about 5.8 rad/s [28]. The peak torque of the actuator, 22 Nm, is capable of providing about 35% of the peak biological knee moment of a male with average weight in the United States [29] during incline walking. The overall range of motion (ROM) of the device is -20 to 90° of knee flexion which covers the full range of walking.

Table 1. Powered knee exoskeleton device specification

Power (W)	70
Max. Continuous Torque (Nm)	11
Peak Torque (Nm)	22
Max. Continuous Speed (rad/s)	4.5
Max. Speed (rad/s)	5.7
Actuator Mass (kg)	1.1
Exoskeleton Mass (kg)	2.7
Range of Motion (°)	-20° to 90° flexion

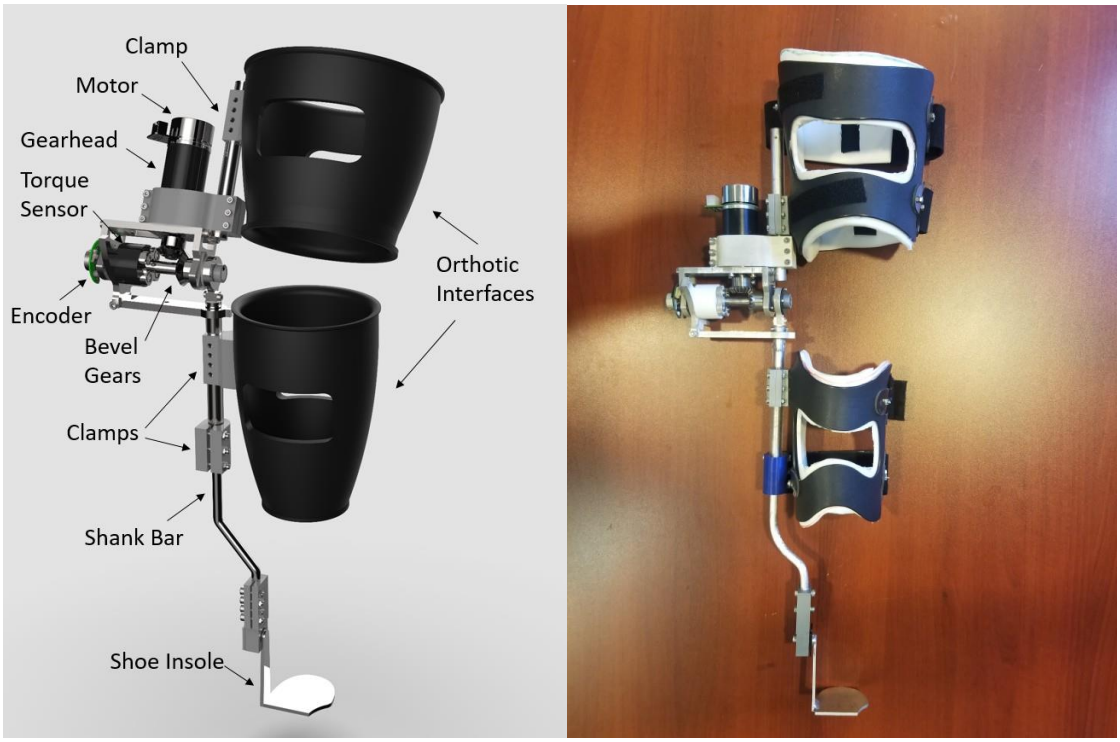

Figure 2.1: Design concept the exoskeleton with key components labeled (left). A prototype of the exoskeleton (right)

2.2 Hardware and Electronics

A unilateral one degree-of-freedom knee exoskeleton is shown in Figure 2.1 An actuator assembly of a brushless DC motor rated for 70W (EC 45 flat, Maxon Motor, Sachsln, Switzerland) and a planetary gearhead (GP42, Maxon Motor, Sachsln, Switzerland) with 113:1 gear reduction was used to provide active power assistance to the user. The direction of the output of the actuator assembly is rotated 90° by a 1:1 gear reduction bevel gear (Misumi, Schaumburg, IL) to align the axis of rotation of the exoskeleton parallel to the axis of rotation of the biological knee joint. A 14-bit resolution absolute rotary encoder (ELS, Ljubljana, Slovenia) was attached to axis of the rotation of the exoskeleton to measure the angular position of the rotation shaft of the exoskeleton. To allow a closed-loop torque control, a reaction torque sensor (Transducer Techniques,

Temecula, CA) was attached to the rotational shaft of the exoskeleton. A 22.2V, 3600 mAh LiPo battery (Venom, Rathdrum, Idaho) powered the exoskeleton and was tethered throughout the experiment. Force sensitive resistors (FSRs) (Interlink Electronics, Camarillo, CA) were attached to the bottom of the AL's foot, as shown in Figure 2.2, and were used to detect the contact between the foot and the ground.

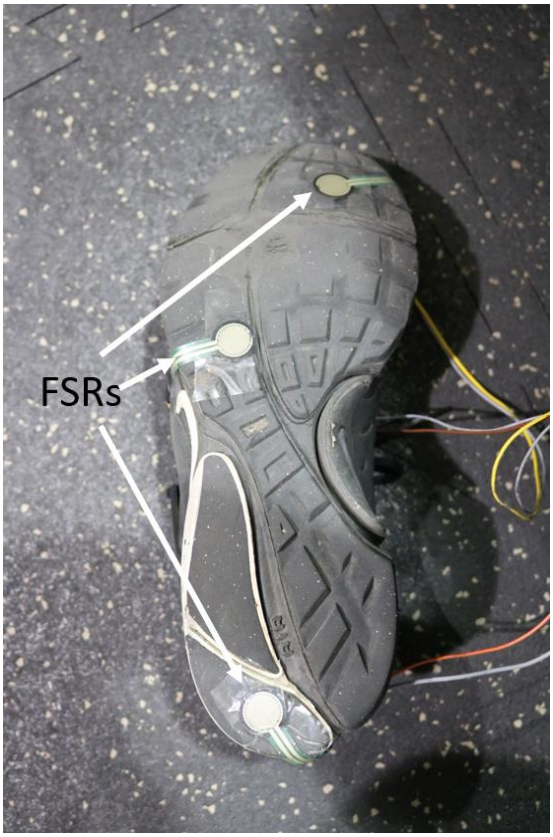

Figure 2.2: The placement locations of FSRs on the bottom of the shoe of the AL. These FSRs were placed front, mid, and button-end of the shoe to detect the heel-contact and toe-off of the foot

Both mid and low-level controls were executed through an NI myRIO 1900 (National Instruments, Austin, Texas). All of the external sensors were integrated by a custom printed circuit board (PCB). Given the shape of the thigh and shank segments, it is difficult to provide enough force against gravity that can hold the position of the

exoskeleton without slipping. To address the issue, a rigid shoe insole was attached to the exoskeleton to provide vertical support for holding up the device. The exoskeleton can accommodate a wide range of body sizes. By adjusting the location of the 3-D printed plastic clamps along the bars, the length of the device can be adjusted to fit the user's thigh and shank lengths by 10 cm to 15 cm, respectively. The height of the device needs to be adjusted for each individual to have the axis of the rotation of the exoskeleton and the axis of the rotation of the user's knee concentrically aligned. This can be achieved with this exoskeleton by changing the vertical position of the shank bar and coupling it with the exoskeleton using a clamp. By doing this, the distance between the shoe insole and the axis of rotation of the exoskeleton can be adjusted from 41 cm to 56 cm. Orthotic interfaces with various sizes allows us to fit a wide range of thigh and shank circumferences. Additionally, tri-density foam was used to provide comfortable and efficient contact between the user's skin and the orthotic interface.

2.3 Device Benchtop Testing

A closed-loop proportional-derivative (PD) torque control to various levels of step inputs was performed to test the device's fidelity of torque tracking. The output position of the actuator stayed fixed throughout the testing. The PD gains were tuned until stable step responses of the system were acquired. Prior to commanding a step input with an absolute magnitude higher than 6 Nm, the actuator was preloaded to 2 Nm for a positive torque and -3 Nm for a negative torque. The benchtop testing on the response of the torque output of the actuator tested the capability of the device to output various levels of torque stably. The actuator was able to successfully output the commanded torque ranging from -8 to 7 Nm as shown in Figure 2.3. The percent overshoot of the step responses was 9.6% for the 8 Nm step input and 11.6% for the 7 Nm step input. The rise times of the step responses to -8 and

7 Nm step inputs were 40ms and 50ms, respectively. The settling time of the step response to -8 Nm step input was 240ms which was greater than the settling time of the step response to 7 Nm step input, 170ms. The steady-state errors for both step responses were within 4%.

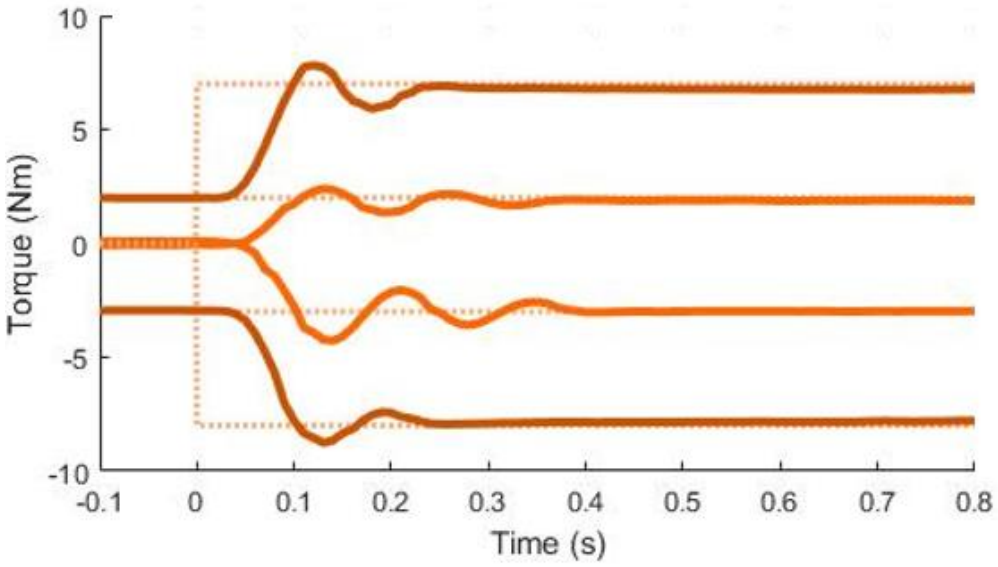

Figure 2.3: Torque PD control testing: The step responses of the actuator to various step inputs ranging from -8 to 7 Nm. The actuator was preloaded to 2 Nm for a 7 Nm step input and -3 Nm for a -8 Nm step input

CHAPTER 3. CONTROL STRATEGY

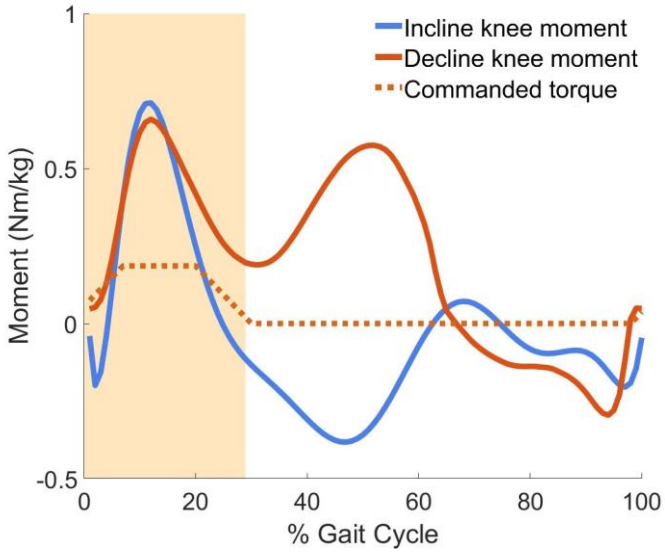

Figure 3.1: Commanded assistance torque vs. biological knee moment during incline and decline walking: The colored region indicates the phase within the gait cycle the assistance is active. Positive moment indicates extension moment, and negative moment indicates flexion moment.

This chapter is dedicated to explaining the control strategy utilized to assist human walking in incline and decline using the knee exoskeleton. Similar to other previous exoskeleton research work for human augmentation [5, 23, 27], the overall control strategy is designed to provide torque assistance to reduce the effort of the targeted joint. In this case, for the knee joint, the controller is designed to provide extension torque assistance during early stance phase. The early stance phase is where the biological knee moment is active in generating an extension moment during both incline and decline walking [13] as shown in Figure 3.1. The whole gait cycle is divided into three different phases. Once the

user's walking phase is determined, the mid-level controller outputs a commanded assistance torque to the low-level controller. The low-level controller tries to match the actual interaction torque between the exoskeleton and the user's knee joint with the commanded assistance torque output. There are two different modes: assistance mode and zero impedance mode. As shown in Figure 3.1, during the assistance mode, the exoskeleton aimed to provide active extension torque assistance during early stance phase and the commanded assistance torque remains 0 Nm throughout the late stance and swing phases. During the zero impedance mode, the commanded assistance torque remained 0 Nm throughout the gait cycle.

3.1 High-Level Control

Using a finite-state machine (FSM), the high-level control determines the phase at which the user is walking. As shown in Figure 3.2, the FSM divided a gait cycle into three different phases: early stance, late stance, and swing phases. During the assistance mode, the early stance phase is the only phase that torque assistance is active. If the current stance phase duration, $Stance\ phase\ duration_i$, exceeds the $Threshold_{i,stance}$, the transition from early stance phase to late stance phase occurs. $Threshold_{i,stance}$ refers to the product of the average duration of the stance phase of the past five strides and a constant. The constant is a tunable value ranging from 0 to 1 that is determined experimentally based on the user's preferred duration of the active assistance. The transition between the late stance and swing phase is determined by the detection of foot contact using FSRs. Measuring the electrical potential across the FSRs and comparing it to a threshold value, $Threshold_{FSR}$, allows for the detection of foot contact. Once the voltage across the FSRs falls below the

Threshold_{FSR}, the system is able to identify that the user's foot is no longer in contact with the ground and that the user has entered swing phase. If the current stride duration, $Stride\ duration_i$, exceeds the $Threshold_{i,stride}$, the transition from swing phase to early stance phase occurs. $\text{Threshold}_{i,\ stride}$ refers to the product of the average stride duration of the past five strides and a constant. The constant is a tunable value ranging from 0 to 1 that was determined experimentally based on the user's preferred assistance onset timing.

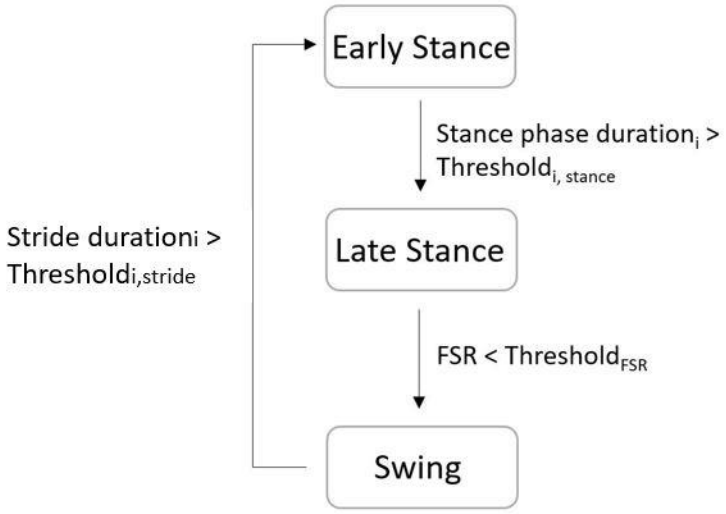

Figure 3.2: Finite State Machine. The finite-state machine is consisted of three different phases. The transition between phases are shown.

3.2 Mid-Level Control

Once the user's walking phase is determined, the magnitude of the commanded assistance torque is determined by the mid-level controller. During the zero impedance mode, the commanded assistance torque remains 0 Nm throughout the gait cycle. However, as shown in Figure 3.3, during the assistance mode, the commanded assistance torque profile aims to provide an extension torque during early stance phase. The commanded

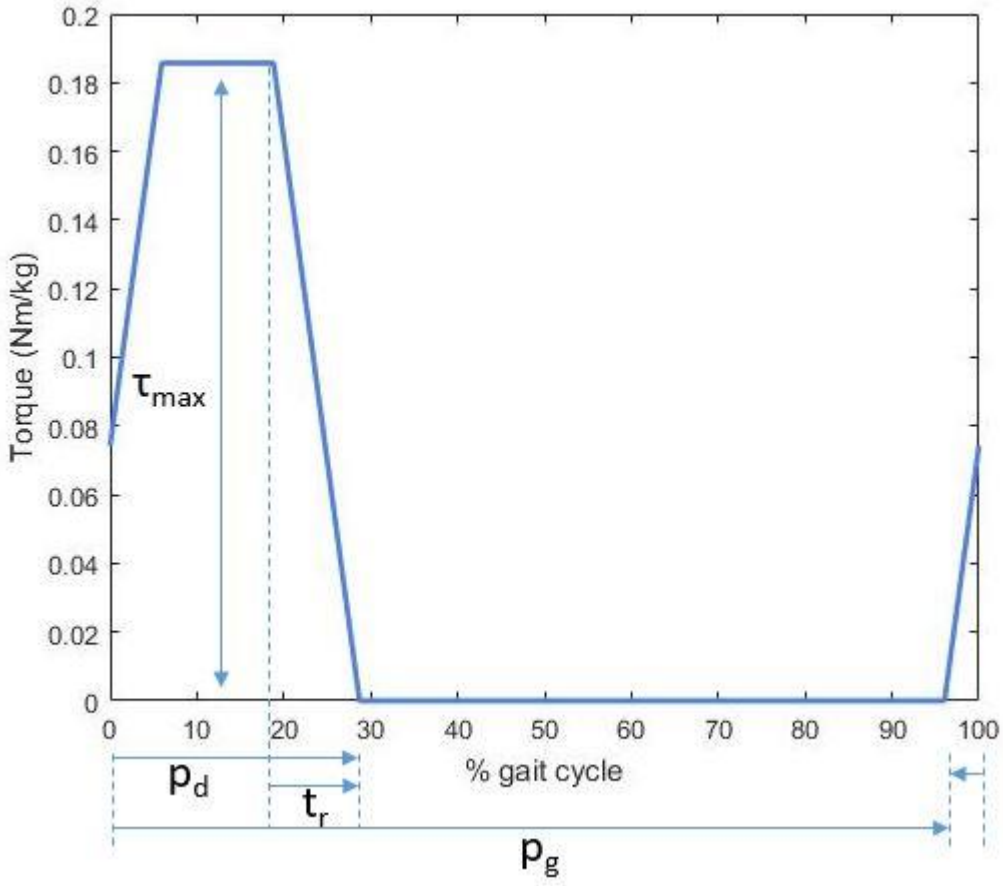

Figure 3.3: A profile of commanded assistance torque: The τ_{max} is the peak commanded torque. The p_g determines the assistance onset timing. The p_d determines the duration assistance. The t_r determines the ramp duration.

assistance torque profile is determined by three different tunable control parameters: p_g, τ_{max}, and p_d. The p_g is a tunable parameter, indicating the percent of the gait cycle at which the torque assistance begins. The length of the gait cycle is estimated as the average duration of the past five strides. The actuator is commanded to initiate providing active torque assistance when the duration of current gait cycle exceeds the product of the estimated gait cycle duration and p_g. τ_{max} is the peak commanded torque for assistance. The commanded assistance torque linearly increases from 0 Nm to τ_{max} for ramp duration, t_r, in the beginning of active assistance period and linearly decreases from τ_{max} to 0 Nm

for t_r at the end of the active assistance period. The p_d determines the duration for which the torque assistance is active. All τ_{max}, p_g and p_d were tuned based on the user's preference with the goal of maximizing the effectiveness of the torque assistance for the subject's walking pattern. The t_r is fixed at 110 ms. The commanded assistance torque is fed into the low-level controller as the desired torque.

3.3 Low-Level Control

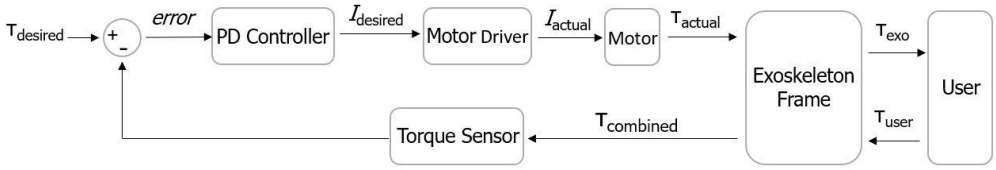

Figure 3.4: The block diagram of the low-level control for a closed loop torque control

When the commanded assistance torque is fed into the low-level controller as the desired torque, the low-level controller aims to match the desired torque and the actual assisted torque from the exoskeleton to the user. The diagram of the closed-loop PD torque controller is shown in Figure 3.4. When a desired torque, $\tau_{desired}$, is commanded, the error is computed by subtracting the current interactive torque, $\tau_{combined}$, read by a torque sensor from $\tau_{desired}$. This error is fed into the PD controller, and the PD controller outputs the desired electrical current output, $I_{desired}$, required to overcome the error. $I_{desired}$ is provided to the motor driver, which allows the motor to draw electrical current, I_{actual}. Using that electrical current, the motor produces torque, τ_{actual}. The difference between the desired torque and the interactive torque is then fed into the PD controller for a closed-loop control. The control loop was updated at 200 Hz.

CHAPTER 4. METHODS

4.1 Experimental Protocol

The study was approved by the Georgia Institute of technology Institutional Review Board, and informed written consent was obtained for all subjects. Twelve healthy adult subjects (9 males/3 females, mean ± SD, age: 22.6 ± 2.7, height: 1.73 ± 0.1 m, mass: 68.9 ± 9.9 kg) without any neurological or gait disorders enrolled in this study. The whole experiment is consisted of two visits. Throughout the visits, the subjects were asked to walk on a force-plate instrumented split-belt treadmill (Bertec Corporation, Columbus, Ohio). The biomechanical effectiveness of torque assistance in early stance phase during walking 15% gradient incline and decline at 0.7 m/s conditions were tested. The first visit was designated for training in walking with the exoskeleton. On the training day, the control parameters in the mid-level controller including maximum assistance torque, τ_{max}, duration of the torque assistance, p_d, and the onset timing of the assistance, p_g, were tuned based on the subject's feedback with the goal of maximizing the effectiveness of the torque assistance for the subject's walking pattern. During tuning process, the baseline values of p_g, τ_{max}, and p_d were 0%, 5 Nm, and 30%, respectively. Each step of change for p_g, τ_{max}, and p_d were 2%, 0.5 Nm, and 2%, respectively. Out of the three tuned control parameters, p_g was tuned first with other two parameters fixed at the baseline level. Tuning was based on the subject's feedback, whether the torque assistance starts too early or too late during stance phase. Next, τ_{max}, was tuned based on the subject's feedback whether the torque assistance is too low or too high with the previously tuned p_g and p_d remaining at the baseline level. After p_g was tuned as the last control parameter based on the subject's feedback whether the assistance duration is too short or too long with the previously tuned p_g and τ_{max}. After all three control parameters were tuned, the subject tried ±2%, ±0.5 Nm

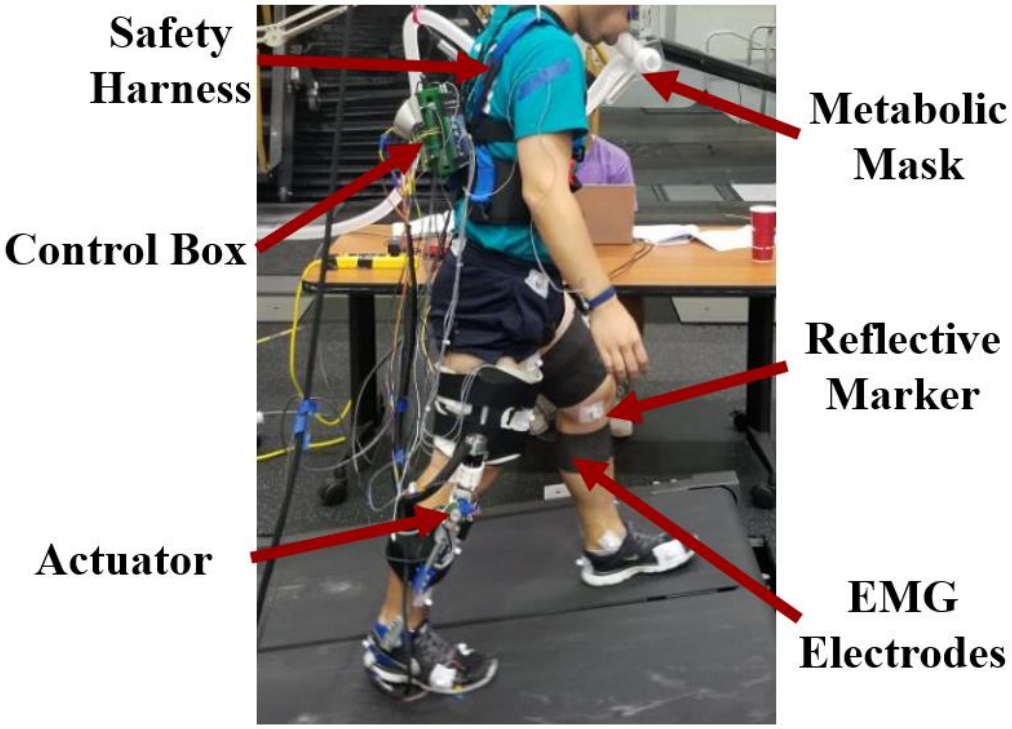

Figure 4.1: Experimental setup during incline walking. Metabolic mask, reflective markers, and EMG electrodes were used for measurement. The subject wore the control box on his/her back. The exoskeleton was put on the subject's right leg.

and ±2% of p_g, τ_{max}, and p_d, respectively, from the tuned control parameters, and the assistance parameters that assisted their walking the most was decided. Lastly, each subject was allowed to walk with the device for approximately 20 minutes in each exoskeleton condition for training purposes. Data collection occurred during the second visit. The experimental setup during data collection is shown in Figure 4.1. In purpose of analyzing the biomechanical effectiveness of the torque assistance to users, the subject's energy expenditure using an indirect calorimetry (Parvo Medics, Sandy, UT), muscle activity using surface electromyography (EMG) electrodes (Biometrics Ltd.), kinematics and kinetics using 3-D motion capture system (Vicon, Oxford, UK) and force- plate instrumented split-belt treadmill, were collected. Before beginning the walking trials,

resting metabolic cost of the subject wearing the exoskeleton was measured for 6 minutes. Prior to the start of data collection for walking trials, subjects were allowed to practice walking with both assistance mode and zero impedance to ensure that they feel comfortable walking with the device. Subjects walked in assistance mode and zero impedance mode for six minutes. Additionally, the subject was asked whether the torque assistance in walking made them feel required less effort than walking without the assistance.

4.2 Data Acquisition and Analysis

During the experiment, the various biomechanical data were collected: metabolic cost, muscle activity, biomechanics, and the user's subjective answer to a qualitative questionnaire were collected.

4.2.1 Metabolic Cost

The measured volume of oxygen uptake and carbon dioxide production were used to calculate the energy expenditure of walking using modified Brockway equation [30]. The resting metabolic cost was subjected from the walking metabolic cost to represent the net metabolic cost of walking. The net metabolic cost for the last two minutes of the six minute trial for each walking conditions was averaged to represent the subject's metabolic cost for each walking mode. Each subject's percent metabolic cost during the assistance mode compare to the subject's zero impedance mode was used for analysis.

4.2.2 Muscle Activity

The muscle activities were collected from six different major muscles acting on the knee joint of AL (n = 12) and UAL (n = 9): vastus lateralis (VL), rectus femoris (RF), vastus medialis (VM), biceps femoris (BF), semitendinosus (ST) and gastrocnemius (GA).

The EMG signal was sampled at 1000 Hz. The raw EMG signal was band-pass filtered between 20 to 400 Hz, full-wave rectified, and, finally, low-pass filtered at 6 Hz to smooth the raw signal. Root mean square average (RMSA) of each muscle's last two minutes of the processed EMG was calculated and compared between the assistance mode and the zero impedance mode for data analysis.

4.2.3 Biomechanics

For data collection, a marker set was created to allow for data collection with the knee exoskeleton. The marker set includes 28 markers in total. The markers are located in the following locations bilaterally: anterior superior iliac spine, posterior superior iliac spine, three markers on the thigh segment, medial knee joint, lateral knee joint, three markers on the shank segment, medial malleolus, lateral metatarsal phalangeal joint, medial metatarsal phalangeal joint, and the posterior calcaneus. The markers on the thigh and shank segments were placed around the knee exoskeleton orthotic on the right leg, then mirrored on the left leg. One of the thigh marker on the AL was placed on the thigh orthotic, and rest of the markers were placed on the user's body. The markers placements listed above were selected to allow for motion capture with the exoskeleton. This marker set was created as a marker template in Vicon to allow for data capture and labeling. Post-processing for kinematics and kinetics data was done in OpenSim. Starting with the Gait2392 model available in OpenSim [31], the model was modified to fit the marker set created in Vicon.

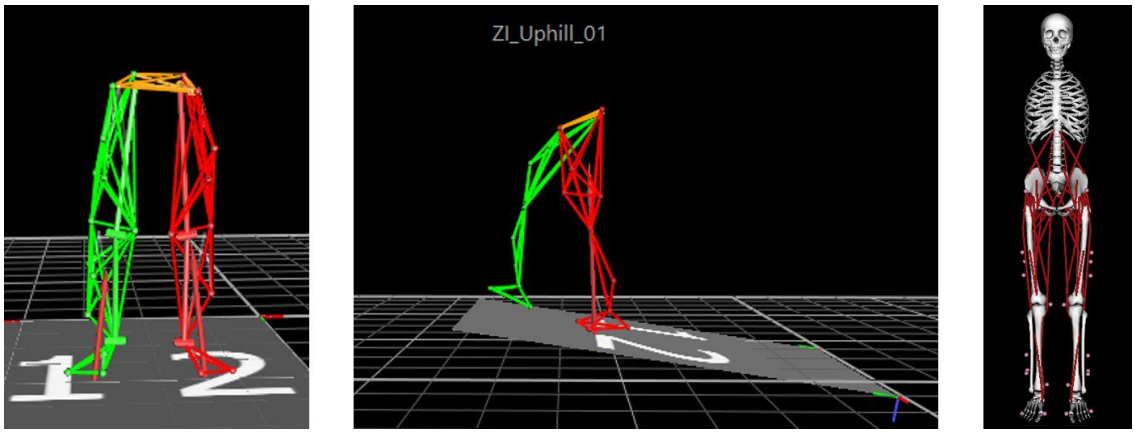

Figure 4.2: The custom-made marker template used on Vicon for marker processing (left and middle), and a model used in OpenSim for processing inverse kinematics and inverse dynamics (right)

The subject's walking in a 3-D space was captured at 1000 Hz using Vicon camera system. The marker data was processed, as shown in Figure 4.2, and low-pass filtered at 6 Hz on the Vicon Nexus software. Then, the marker data, sampled at 200 Hz, was combined with the ground reaction force data from the force-plate, sampled at 1000 Hz, to perform sagittal-plane inverse dynamics in OpenSim, as shown in Figure 4.2. The last two minutes of biomechanics data of each of six-minute walking trials were analyzed. The heel-contact and toe-off was detected by comparing the ground-reaction force in the vertical direction with 40 N as a threshold. The kinetic contribution of the exoskeleton to the knee joint on AL was subtracted from the output kinetic data of the knee joint from inverse dynamics analysis to represent the biological effort the knee produced. The biomechanics data were collected on eight subjects. One subject's biomechanics during incline was excluded due to poor marker tracking performance during post processing.

4.2.4 User Preference

After finishing walking on each slope, the subjects were asked whether the assistance provided during the assistance mode help them walk with less effort. The users provided their subjective answer to the question in a scale from 1 to 10 where 1 is strongly disagree and 10 is strongly agree.

4.2.5 Spatio-Temporal Parameters

The percent stance phase was calculated by dividing the stance phase duration by the duration of the gait cycle. The stride length was calculated as the time duration from one heel contact to the next heel contact of the same leg. Symmetry index is calculated as the ratio of the percent stance phase of the AL to the percent stance phase of the UAL [32]. A symmetry index close 100% indicates symmetric gait.

4.2.6 Statistical Analysis

A paired t-test was used to test the significance of the difference in quantities including muscle activity, kinetics, and kinematics between the assistance mode and the zero impedance mode with a $p < 0.05$ criterion. A regression analysis was run between the percent change in metabolic cost and the user preference for incline walking and decline walking separately.

CHAPTER 5. RESULTS

This chapter is dedicated for presenting the result from the experiment. This chapter is broken into six different sections: user preference and metabolic cost, commanded assistance torque profiles and device torque tracking performances, muscle activity, kinetics, kinematics, and spatio-temporal parameters. The results in each section are divided into incline walking and decline walking.

5.1 User Preference & Metabolic Cost

Before starting this experiment, it was expected that a metabolic reduction in the assistance mode compared from zero impedance mode would be prevalent. However, in the post-hoc data processing, metabolic reduction across subjects was not consistently present. Therefore, we defined a subject as a responder if the subject exhibited a reduction in net metabolic cost greater than 1.0% during assistance mode when compared to his/her net metabolic cost during zero impedance mode. The nonresponder was defined as a subject who increased his/her net metabolic cost or reduced net metabolic cost less than 1.0% during assistance mode compared to his/her net metabolic cost during zero impedance mode. There were only six responders in incline walking and seven responders in decline walking as shown in Table 5.1. Consequently, it was sought to identify the biomechanical cause(s) of the inconsistency in the presence of the metabolic reduction across the subjects. For this purpose, each section in this chapter is presented as the responders versus nonresponders and/or across subjects.

Table 5.1: The percent change in metabolic cost with assistance and user preference. The percent changes in metabolic cost in the assistance mode from zero impedance mode and user preferences in incline and decline walking are shown for each subject. Each subject was asked "Did the assistance help you walk with less effort?" The percent changes in metabolic cost greater than 1% are bolded.

	Δ metabolic cost in incline (%)	Did the assistance in the incline help you walk with less effort?	Δ metabolic cost in decline (%)	Did the assistance in the decline help you with walk less effort?
Subject 1	**-6.4**	8	**-7.6**	7
Subject 2	**-4.5**	8	10.1	8
Subject 3	-0.1	10	**-1.1**	10
Subject 4	1.3	8	**-4.3**	7
Subject 5	4.4	6	-0.7	4
Subject 6	**-3.1**	9	3.5	9
Subject 7	**-3.5**	9	**-19.3**	8
Subject 8	**-2.6**	10	**-3.1**	2
Subject 9	0.4	8	18.9	7
Subject 10	**-1.6**	8	**-7.0**	8
Subject 11	3.7	10	**-10.3**	10
Subject 12	5.1	8	22.6	9

5.1.1 Incline

In incline walking, the subjects generally felt that they were using less effort during the assistance mode compared to zero impedance mode based on their subjective answers (mean ± sem: 8.5 ± 0.4). There was no rating below 5, nor agree or disagree, on the question

asked for incline walking. The user preference did not correspond to the percent change in metabolic cost with assistance in incline walking ($p = 0.51$).

Six of the twelve were incline responders. As shown in Table 5.2, during incline walking, the responders averaged 3.6% metabolic reduction with the torque assistance. The incline nonresponders exhibited 2.5% metabolic increase on average. There was no noticeable difference in the answer to the question between the responders and nonresponders in incline walking (responders: 8.7 ± 0.3, nonresponders: 8.33 ± 0.6).

Table 5.2: Average percent change in metabolic cost between the assistance mode and zero impedance mode during both incline and decline. A negative number indicates reduction of the metabolic cost with the assistance using the exoskeleton. Mean (± SEM).

	Incline responders	Incline nonresponders	Decline responders	Decline nonresponders
Average Δ metabolic cost (%)	-3.6 (± 0.8)	+2.5 (± 0.9)	-7.5 (± 2.3)	+10.9 (± 4.4)

5.1.2 Decline

In decline walking, two subjects disagreed with the statement that it required less effort to walk in the assistance mode, compared to zero impedance mode. One of these subjects was a responder, and the responder subject commented that he/she felt the hip joint on the AL had to "work more" when assistance was provided. The other subject that disagreed was a non-responder, simply stating assistance mode "took more effort." The user preference did not correspond to the percent change in metabolic cost with assistance

in decline walking (p = 0.85). As shown in Table 5.2, seven of the twelve subjects were decline responders with an average of 7.5% metabolic reduction. The five decline nonresponders increased metabolic cost by 10.9%. No difference was observed between the responders and nonresponders group's answer to the question in decline walking (responders: 7.4 ± 0.4, nonresponders: 7.4 ± 0.4).

5.2 Commanded Assistance Torque Profiles & Device Torque Tracking Performances

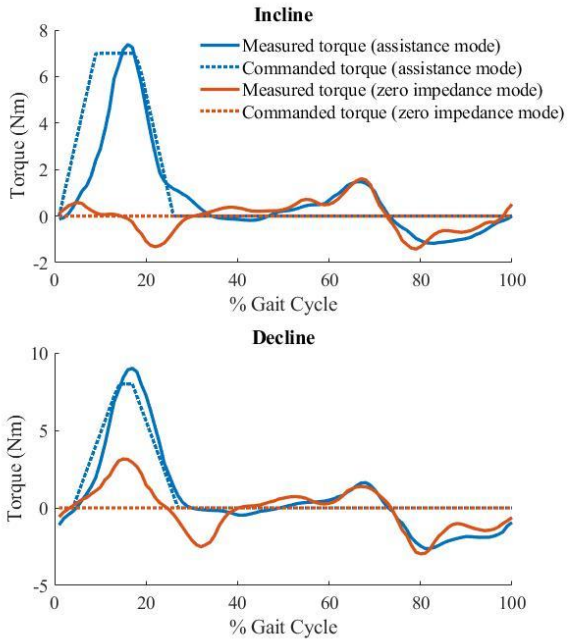

Figure. 5.1: A representative torque tracking during assistance mode and zero impedance mode for both incline and decline walking. The root mean square error (RMSE) of the torque tracking was 1.21 Nm during incline assistance mode, 0.69 Nm during incline zero impedance mode, 1.27 Nm during decline assistance mode, and 1.43 Nm during decline zero impedance mode.

A representative torque tracking during the assistance mode and zero impedance in incline and decline walking are shown in Figure 5.1. The RMSE of torque tracking during the assistance mode was very consistent during the assistance mode in incline and decline walking. However, the RMSE during zero impedance mode in decline walking was particularly larger than in incline walking due to a high collisional effect from the ground contact during early stance phase in decline walking.

Table 5.3: Average commanded maximum torque, percent stance phase duration of assistance, and percent of the gait cycle assistance onset point for all subjects, responders, and nonresponders during incline and decline walking. Mean (±SEM)

	Incline all subjects (n = 12)	Incline responders (n = 6)	Incline nonresponders (n = 6)	Decline all subjects (n = 12)	Decline responders (n = 7)	Decline nonresponders (n = 5)
τ_{max} (Nm)	10.0 (±0.5)	10.3 (±0.5)	9.8 (±0.8)	8.5 (±0.9)	8.6 (±1.1)	8.5 (±0.7)
p_d (%)	43.2 (±1.7)	42.3 (±1.3)	44.0 (±2.2)	42.3 (±1.2)	42.1 (±1.2)	42.6 (±1.7)
p_g (%)	99.8 (±0.9)	98.2 (±0.8)	101.5 (±0.3)	100.8 (±0.6)	100.3 (±1.0)	101.4 (±0.7)

5.2.1 Incline

Referring to Table 5.3, across all subjects, the mean commanded maximum torque, τ_{max}, during incline assistance mode was 10.0 ± 0.5 Nm. The percent duration of the active torque assistance during stance phase, p_d, averaged 43.2 ± 1.7 % of the stance phase duration. Most of the subjects preferred the onset point of the assistance, p_g, near the heel-contact during incline assistance mode. There was no noticeable differences in p_d and τ_{max}

between the responders and nonresponders. The average p_g for the responders was earlier than the average p_g for the nonresponders by 3.3%.

5.2.2 Decline

During decline assistance mode, the average τ_{max} across the subject group was 8.5 ± 0.9 Nm, which was about 1.5 Nm lower than the average τ_{max} during the incline assistance mode across the subject group. Both average p_d and p_g during decline assistance mode were pretty consistent with the average p_d and p_g during incline assistance mode. The τ_{max}, p_d and p_g during decline assistance mode show no large difference between the responders and nonresponders.

5.3 Muscle Activity

5.3.1 Incline

As shown in Figure 5.2, across all subjects in incline walking, the muscles that exhibited statistically significant change in their muscle activity in the assistance mode compared to zero impedance mode were the knee extensors on the AL and the ankle planterflexor of the UAL: VL 10.5 ± 3.8% reduction ($p < 0.05$), RF 9.6 ± 2.1% reduction ($p < 0.001$), VM 10.9 ± 2.1% reduction ($p < 0.001$), GA 5.6 ± 2.3% increase ($p < 0.05$). On the AL, even though it was not statistically significant, ST increased activation 10.0 ± 5.1% ($p = 0.075$).

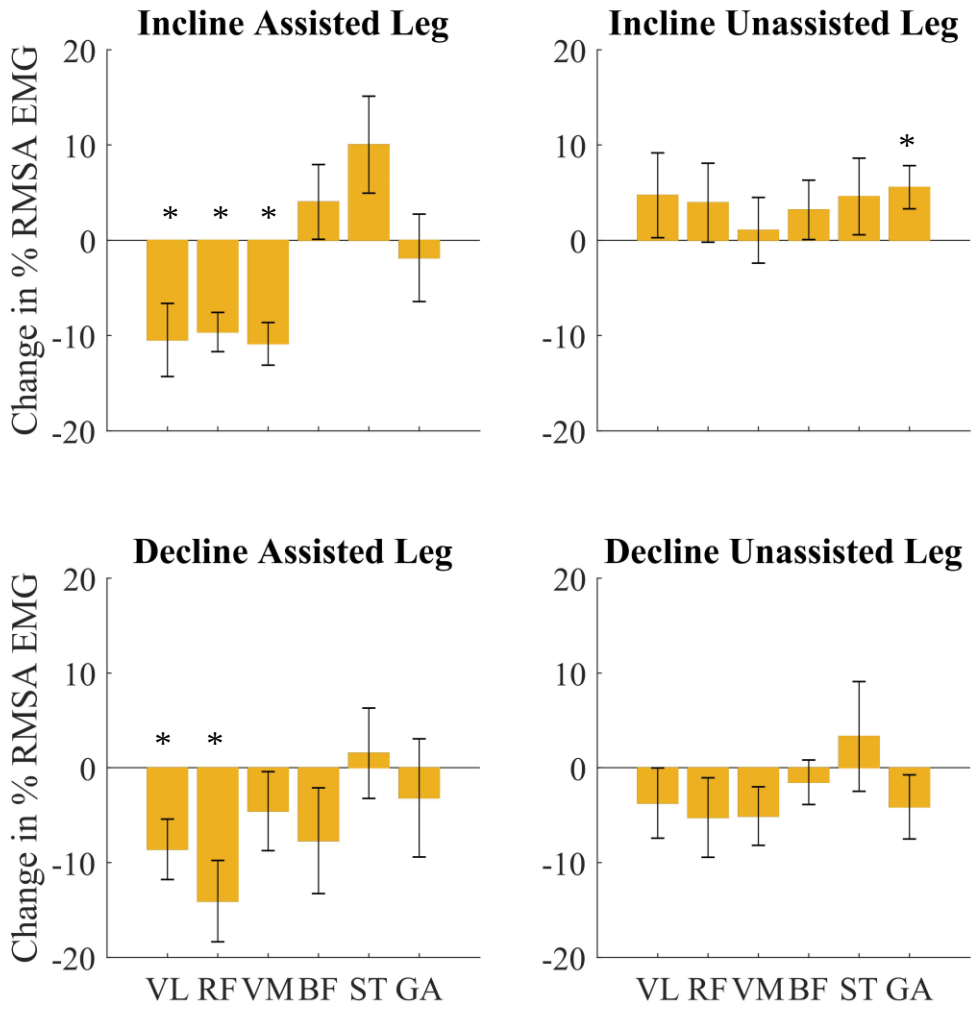

Figure 5.2: Comparison in the average percent RMSA EMG change in both AL (left column) and UAL (right column) across all subjects during the assistance mode compared to the zero impedance mode in incline (top row) and decline walking (bottom row). The stars (*) indicate statistically significant changes.

The average percent change in RMSA of each muscle on both AL and UAL of responders and nonresponders in incline and decline walking are shown in Figure 5.3. Both

the responders and nonresponders during incline walking have shown a similar trend in the change of muscle activation level of the muscles around the knee joint on the AL. The reduction in muscle activation of the knee extensors on the AL were commonly present in both the responders and nonresponders groups. However, the magnitude of the responders' knee extensor activation reduction was much greater than the nonresponders' knee extensor activation reduction (almost times 2 for each of the knee extensors). The hamstring muscle activation on the AL also increased with the assistance for both responders and nonresponders. Especially, the activation of the responders' ST on the AL increased 27.1 ± 4.5% with the assistance when the nonresponders' increase was 7.5 ± 5.5%. The change in muscle activation level of the muscles on the UAL showed a large difference between the responders and nonresponders during incline walking. Notably, the nonresponders increased all of UAL's knee extensor muscle activation: VL 8.7 ± 7.8% increase, RF 6.1 ± 6.6% increase, and VM 6.2 ± 4.8% increase. However, the responders did not show a consistent increase in the knee extensors' muscle activation where VL remained almost unchanged, VM reduced 5.6 ± 2.9% and RF increased 1.2 ± 5.0%.

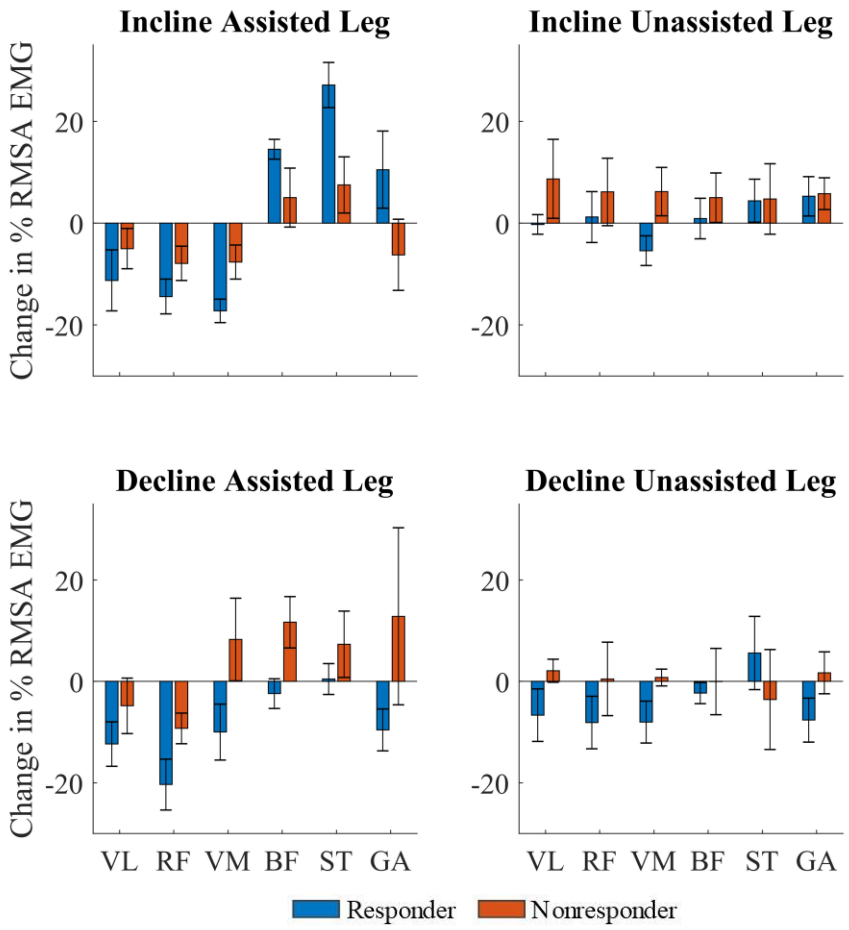

Figure 5.3: Average percent change in RMSA EMG on AL (left column) and UAL (right column) of responders and nonresponders during the assistance mode compared to the zero impedance mode in incline and decline walking.

5.3.2 Decline

As shown in Figure 5.3, the extension torque assistance during weight acceptance of the gait cycle in decline walking significantly reduced activation in a majority of the knee extensors: VL 8.6 ± 3.8% reduction ($p < 0.05$) and RF 14.1 ± 4.3% reduction ($p <$

0.01). VM also reduced its activation with the assistance by 4.6% ± 4.2% with no significance (p = 0.29).

Similar to the difference between the responders and nonresponders knee extensor muscle activation of the AL during incline walking, both responders and nonresponders exhibited reduction of the AL's VL and RF activation level in decline walking. However, the reduction of the responders' (VL 12.5 ± 4.4%, RF 20.4 ± 5.0%) was larger than that of the nonresponders' (VL 4.8 ± 5.5%, RF 10.8 ± 3.0%). However, the nonresponders' VM on the AL increased activation (8.3 ± 8.2%) with assistance, whereas the responders' decreased (10.0 ± 5.5%). During decline walking, the responders generally reduced muscle activation of all of the knee extensors of the UAL (VL 6.7 ± 5.2%, RF 8.1 ± 5.1%, and VM 8.0 ± 4.1%). On the other hand, the nonresponders presented a slight increase in muscle activation in all of the knee extensor muscles (VL 2.1 ± 2.2%, RF 0.5 ± 7.2%, VM 0.8 ± 1.7%).

5.4 Kinetics

5.4.1 Incline

As shown in Figure 5.4, across all subjects, the knee on the AL decreased the joint's positive power generation by 18.4 ± 10.5% with the assistance compare to zero impedance mode without statistical significance (p = 0.13). The responders commonly reduced the positive work generation at all of the lower-limb joints on both legs in the assistance mode. Especially, the assistance substantially reduced the positive power generation of the knee on the AL per stride by 0.038 W/kg, equivalent to 33.5% averaged reduction compare to zero impedance mode (0.092 W/kg for the assistance mode, 0.130 W/kg for the zero

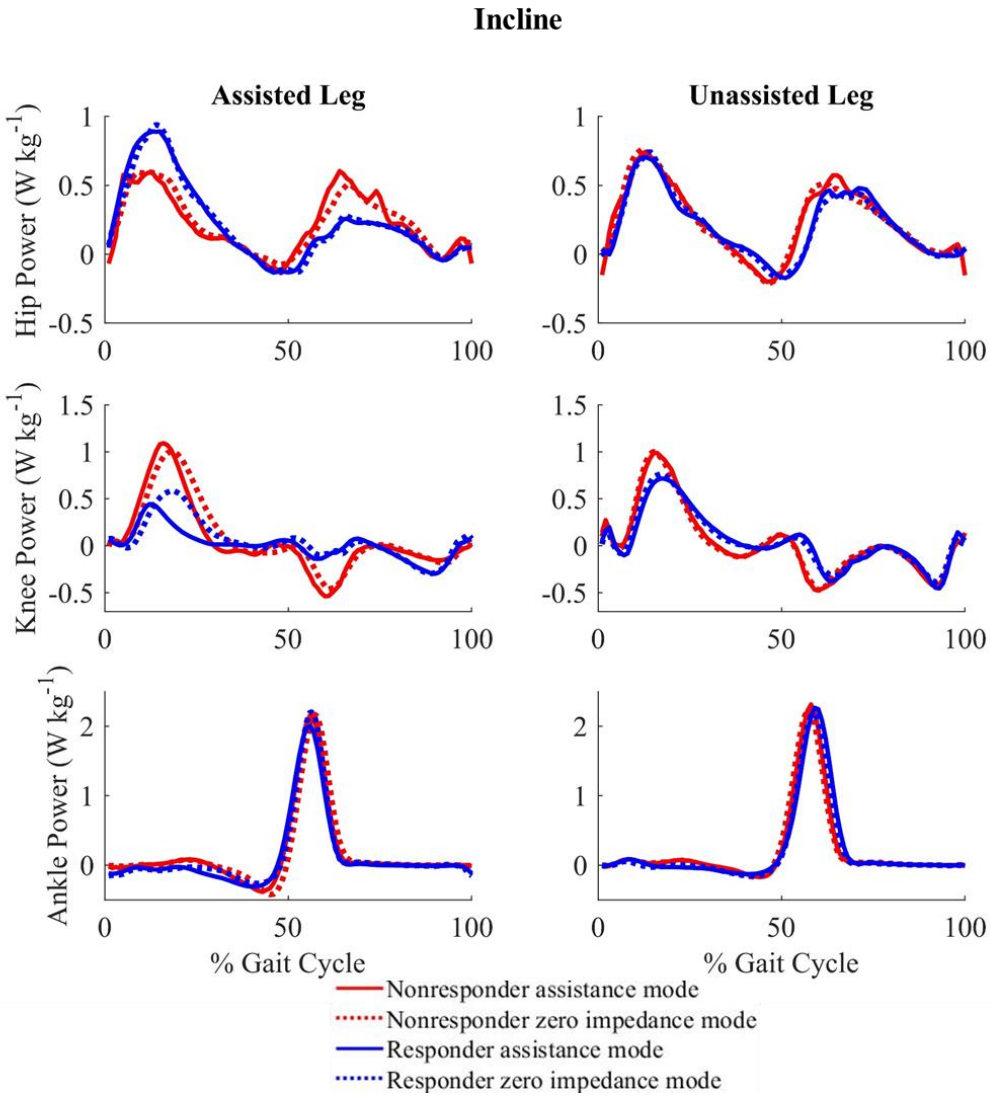

Figure 5.4: The biological power profile of hip, knee, and ankle joints in the sagittal plane of the responders (blue) and the nonresponders (red) during incline walking. The AL is plotted on the left column, and the UAL is plotted on the right column. The solid line: assistance mode. The dotted line: zero impedance mode.

impedance mode). The nonresponders minimally reduced the positive power generation of the knee joint on the AL by 0.004 W/kg with the assistance (0.171 W/kg for assistance mode and 0.175 W/kg for zero impedance mode). Interestingly, during the assistance

mode, the responders' positive power of the knee joint on the UAL was decreased by 3.2% compare to zero impedance mode. In parallel to the increase of the UAL's knee extensors EMG, the nonresponders' knee joint of the UAL increased positive power by 14.0% on average. The responders reduced the total positive power from all lower-limb joints on both legs combined during assistance mode compared to zero impedance mode by 2.6% when nonresponders showed an increase by 2.3%.

5.4.2 Decline

The biological joint power profiles of the AL and UAL during decline assistance mode and zero impedance mode are plotted in Figure 5.5. Decline walking is marked by a substantial amount of power absorption at lower-limb joints [12]. The extension torque assistance at the knee during the assistance mode was intended to assist negative power absorption at the knee joint during the weight acceptance phase. With the assistance, the subjects' response in the knee negative power absorption largely varied. In average across all subjects, the magnitude of the biological negative power absorption at the knee increased 10.9% ± 8.9% with assistance mode compare to zero impedance mode.

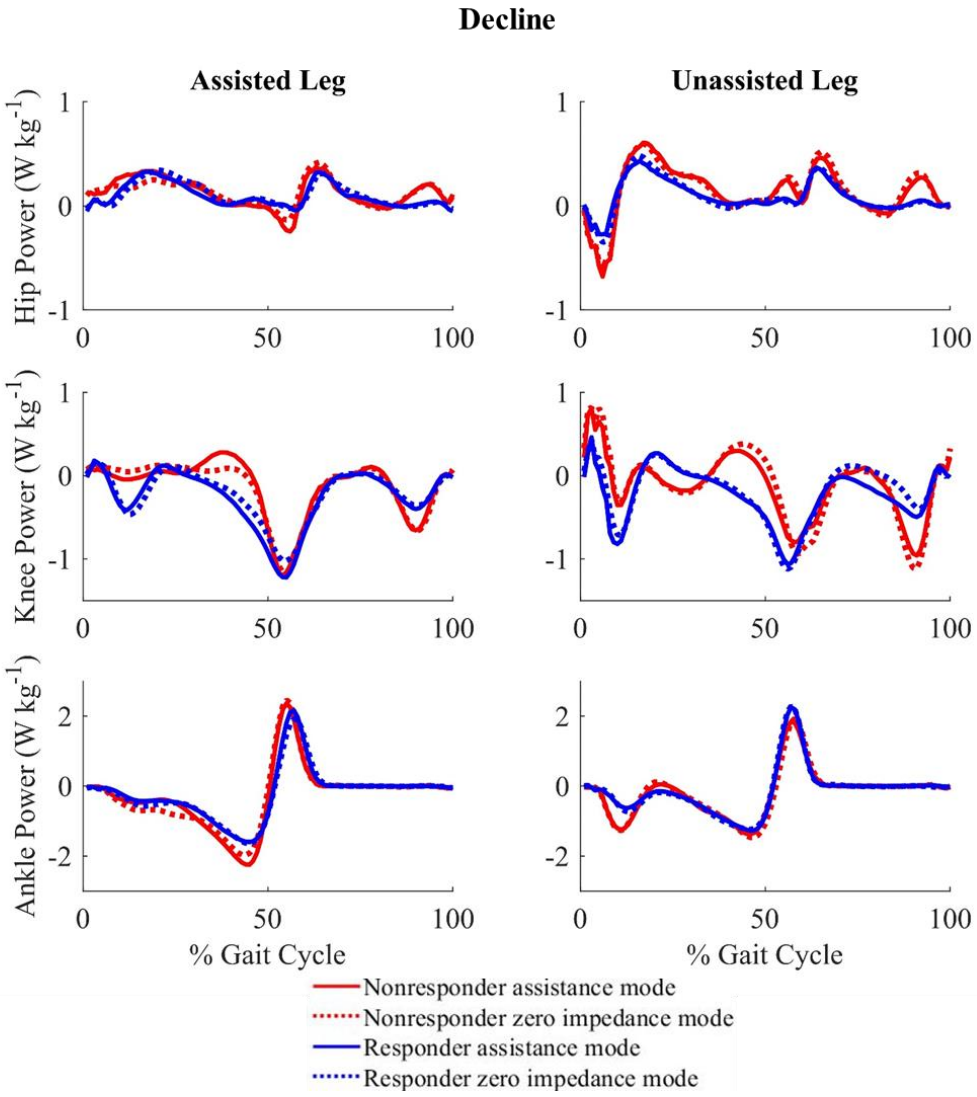

Figure 5.5: The biological power profile of hip, knee, and ankle joints in the sagittal plane of the responders (blue) and the nonresponders (red) during decline walking. The AL is plotted on the left column, and the UAL is plotted on the right column. The solid line: assistance mode. The dotted line: zero impedance mode.

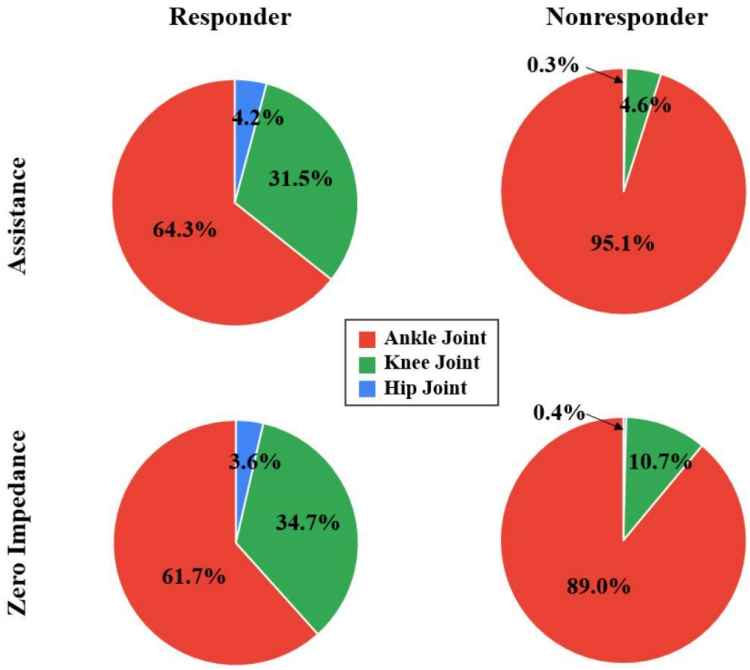

Figure 5.6: Averaged percent distribution of each joint's negative power absorption to the total negative power absorption of the assisted side during the first 25% of gait cycle (the power input from the exoskeleton is included on the knee joint and the total negative power of the leg).

The first 25 percent of gait cycle was where the extension torque assistance was mostly active and the lower-limb joints heavily respond to translating the weight of the body from the contralateral leg by creating negative power During the zero impedance mode, the responders' average power absorption on the AL over the first 25% of gait cycle was -0.55 ± 0.05W/kg, and the nonresponders' was -0.52 ± 0.10 W/kg. However, the contribution of each joint to the total negative power was different between the responders and nonresponders as shown in Figure 5.6. During the first 25 percent of the gait cycle in the zero impedance mode, the total negative power absorption from all lower-limb joints including the power input of the exoskeleton on the nonresponders' AL was heavily relying

on their ankle. The ankle joint solely producing 95.1% ± 4.5% of the total negative power absorption of the AL including the power input of the exoskeleton. Consequently, the knee's contribution to the total power absorption over the phase was minimal. The knee joint of the assisted side contributed only 4.6% ± 4.5% of the total negative power absorption of the AL including the power input of the exoskeleton. On the other hand, the responders utilized their knee much more by absorbing 31.5% ± 4.8% of the total negative power of the assisted side over the first 25% of the gait cycle. Simultaneously, the responders' ankle joint on the AL have shown a relatively lower contribution to the total negative absorption of the assisted side during zero impedance mode compared to nonresponders' ankle contribution to the total negative power of the assisted side during zero impedance mode. This was also apparent in the absolute W/kg scale. On average, the nonresponder group's knee joint during the first 25 percent of decline zero impedance mode was absorbing only -0.03 W/kg. On the other hand, the knee joint on the AL of the responders were absorbing energy at the rate of -0.19 W/kg. During the assistance mode in decline, both the responders and nonresponders increased the percent contribution of the knee joint to the total negative power of the AL compared to the percent contribution of the joint to the total negative power of the AL during the zero impedance mode.

5.5 Kinematics

5.5.1 Incline

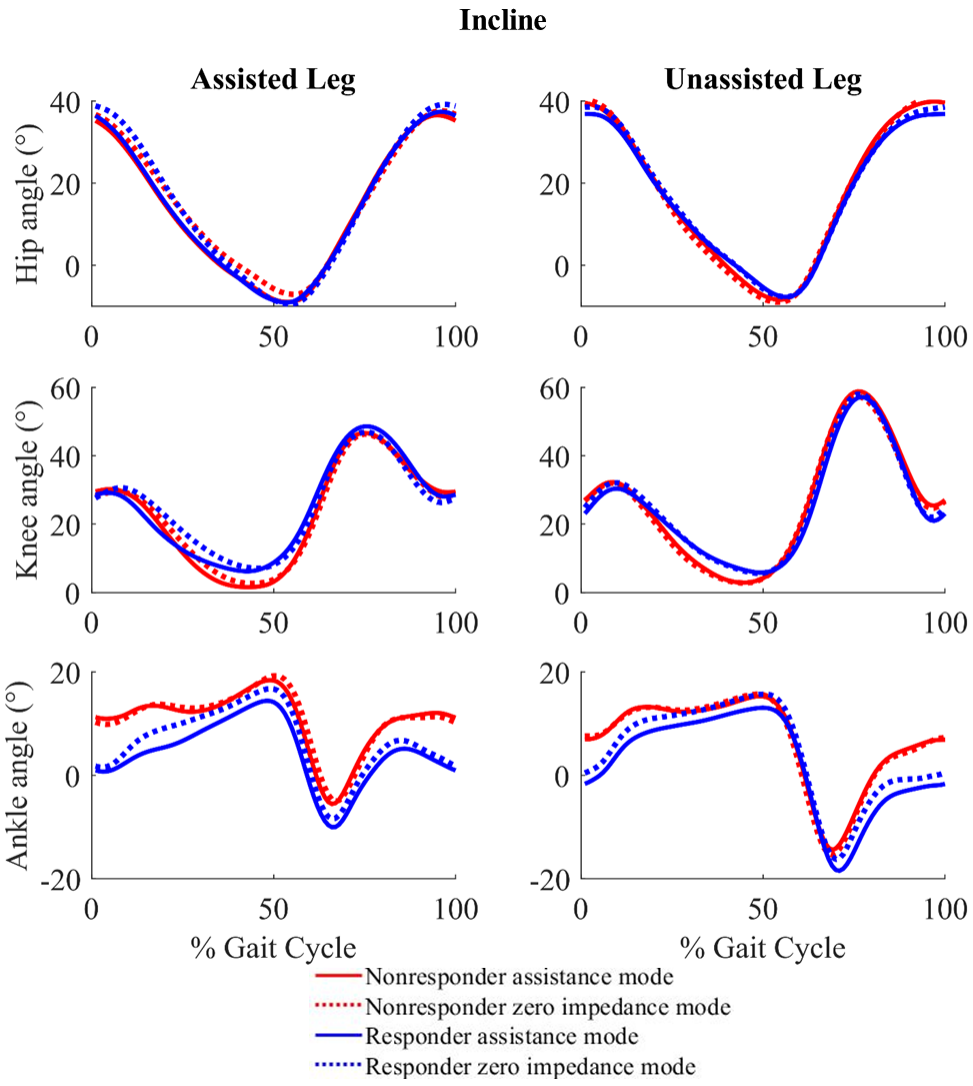

Figure 5.7: The kinematic profile of hip, knee, and ankle joints in the sagittal plane of the responders (blue) and the nonresponders (red) during incline walking. The AL is plotted on the left column, and the UAL is plotted on the right column. The solid line: assistance mode. The dotted line: zero impedance mode

Table 5.4. Average ROM of the hip, knee, and ankle joints in sagittal plane during incline walking. Mean (±SEM)

		Incline responders		Incline nonresponders	
		Assistance mode	Zero impedance mode	Assistance mode	Zero impedance mode
AL	Hip (°)	47.4 (±2.1)	50.0 (±1.8)	47.3 (±2.4)	46.5 (±2.5)
	Knee (°)	43.4 (±2.3)	40.8 (±2.8)	47.2 (±3.4)	45.5 (±3.7)
	Ankle (°)	28.5 (±4.7)	29.1 (±2.2)	26.5 (±5.1)	27.0 (±2.1)
UAL	Hip (°)	46.2 (±1.8)	48.4 (±0.8)	51.8 (±1.7)	52.5 (±5.8)
	Knee (°)	52.9 (±2.9)	53.8 (±2.4)	57.4 (±2.2)	55.8 (±4.9)
	Ankle (°)	33.9 (±1.4)	34.2 (±1.8)	32.6 (±2.0)	34.2 (±3.7)

The average ROM of the hip, knee, and ankle joints in sagittal plane during incline walking are shown on Table 5.4. The knee ROM of the AL during the assistance mode increased from the zero impedance mode (responders +2.6° increase, nonresponders +1.7° increase). The knee ROM of the responders in both legs were relatively smaller than the nonresponders'. The change in the ankle ROM between the assistance mode and zero impedance was consistently small in both legs and both groups. The nonresponders were exhibited larger maximum extension angle at the knee during stance phase than the responders on both legs. The maximum knee extension angle of the AL of the responders

were 5.8° and the maximum knee extension angle of the AL of the nonresponders were 0.4°.

5.5.2 Decline

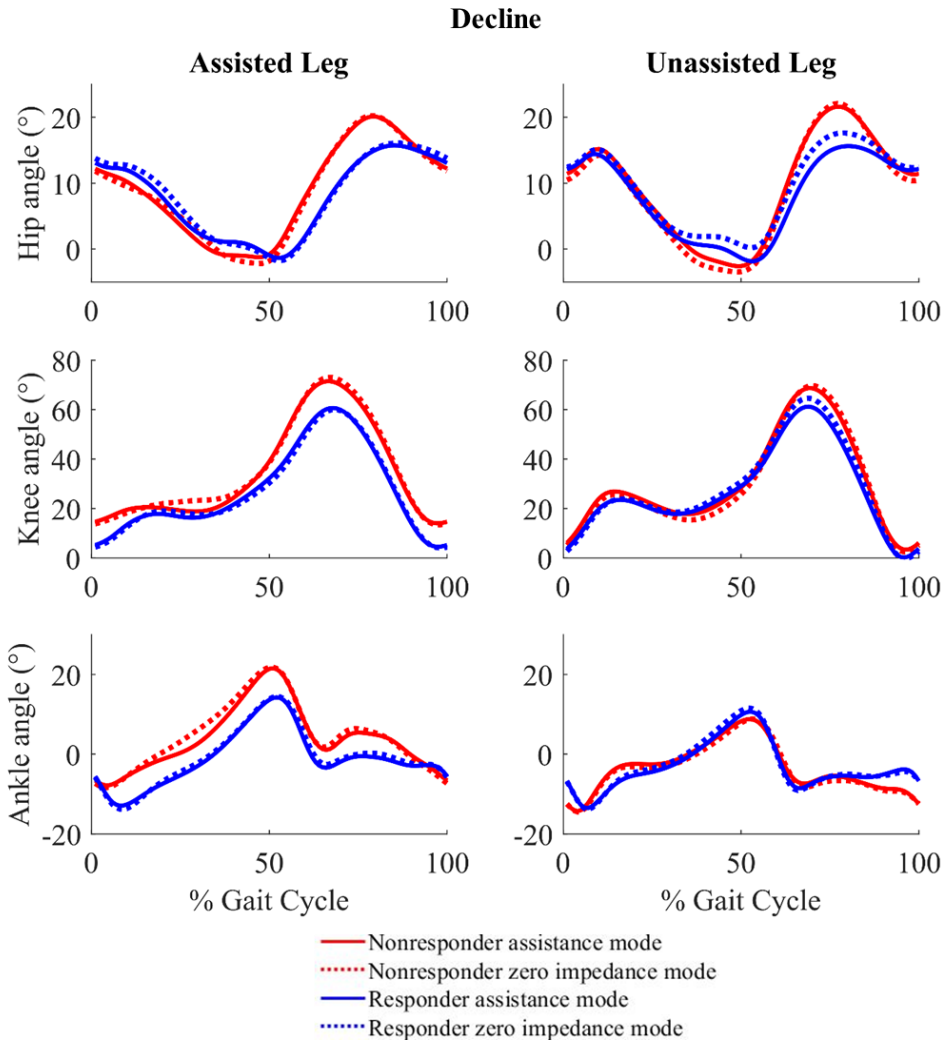

Figure 5.8: The kinematic profile of hip, knee, and ankle joints in the sagittal plane of the responders (blue) and the nonresponders (red) during decline walking. The AL is plotted on the left column, and the UAL is plotted on the right column. The solid line: assistance mode. The dotted line: zero impedance mode

Table 5.5: Average ROM of the hip, knee, and ankle joints in sagittal plane during decline walking. Mean(±SEM)

		Decline responders		Decline nonresponders	
		Assistance mode	Zero impedance mode	Assistance mode	Zero impedance mode
AL	Hip (°)	18.4 (±1.4)	19.1 (±1.8)	22.3 (±4.0)	23.1 (±1.6)
	Knee (°)	57.9 (±1.9)	58.4 (±2.8)	58.4 (±9.5)	60.5 (±8.3)
	Ankle (°)	30.8 (±2.7)	31.4 (±2.2)	30.2 (±2.9)	30.9 (±3.7)
UAL	Hip (°)	21.0 (±1.4)	20.5 (±0.8)	24.5 (±0.4)	26.1 (±1.0)
	Knee (°)	62.4 (±2.5)	66.5 (±2.4)	66.2 (±2.6)	67.9 (±2.5)
	Ankle (°)	27.5 (±1.2)	29.1 (±1.8)	23.9 (±0.4)	23.4 (±1.0)

The average ROM of the hip, knee, and ankle joints in sagittal plane during decline walking are shown on Table 5.5. The knee ROM of the AL during the assistance mode increased from the zero impedance mode (responders +2.6° increase, nonresponders +1.7° increase). The change in the ankle ROM between the assistance mode and zero impedance was consistently small in both legs and both groups.

5.6 Spatio-temporal parameters

5.6.1 Incline

Table 5.6: Incline walking spatio-temporal parameters. Mean(±SEM)

	Incline responders		Incline nonresponders	
	Assistance mode	Zero impedance mode	Assistance mode	Zero impedance mode
AL % stance phase	60.3 (±0.3)	61.5 (±0.2)	60.6 (±0.6)	60.8 (±0.7)
UAL % stance phase	65.0 (±0.1)	64.4 (±0.2)	63.3 (±0.5)	60.4 (±0.9)
Symmetry index (%)	92.7 (±0.5)	95.5 (±0.2)	95.7 (±0.5)	100.8 (±0.6)
Stride frequency (strides/min)	42.6 (±0.5)	40.4 (±0.8)	43.2 (±1.6)	42.1 (±1.5)
Stride length (mm)	986.8 (±11.2)	1039.8 (±20.2)	972.5 (±33.6)	999.1 (±31.3)

The symmetry index is the ratio between the percent stance phase of the AL and UAL. Based on the symmetry index, the responders were walking more asymmetrically during the zero impedance mode compared to the nonresponders as shown in Table 5.6. This was largely caused by the large percent stance phase of the responders' UAL. The assistance caused more asymmetric gait for both responders and nonresponders. The percent stance phase was decreased with the assistance for the responders compare the percent stance phase during zero impedance mode whereas the nonresponders' almost remained unchanged between the two modes. The assistance also increased the cadence for both responders and nonresponders.

5.6.2 Decline

Table 5.7: Decline walking spatio-temporal parameters. Mean(±SEM)

	Decline responders		Decline nonresponders	
	Assistance mode	Zero impedance mode	Assistance mode	Zero impedance mode
AL % stance phase	61.9 (±0.3)	61.2 (±0.4)	58.8 (±0.8)	58.8 (±0.4)
UAL % stance phase	62.0 (±0.1)	61.1 (±0.1)	58.7 (±1.9)	62.3 (±0.5)
Symmetry index	99.8 (±0.5)	100.2 (±0.8)	100.2 (±2.1)	94.4 (±0.2)
Stride frequency (strides/min)	47.9 (±0.7)	47.5 (±0.7)	56.5 (±1.4)	56.8 (±1.8)
Stride length (m)	877.4 (±12.6)	883.3 (±13.7)	743.8 (±20.7)	740.2 (±25.7)

Based on the symmetry index, the nonresponders were walking more asymmetrically during the zero impedance mode compared to the responders as shown in Table 5.7. Unlike incline walking, the assistance caused more symmetric gait for the nonresponders during decline walking. The trend in the change of cadence with assistance was not consistent between the responders and nonresponders.

CHAPTER 6. DISCUSSION

Across all subjects, the knee extension torque assistance during incline walking was effective in producing a significant reduction on the muscle activation of all three knee extensor muscles (VL, RF, VM) of the AL as well as with no significant changes of the muscle activation of the knee extensors on the UAL. However, the hamstring muscles of the AL have shown increase of activation with assistance without statistical significance. This may indicate that the users' knee flexors may have fought against the knee extension assistance. The extension assistance was also effective in significantly reducing the muscle activation in the VL and RF of the AL in decline walking. Therefore, the first hypothesis is accepted in both incline and decline walking. The reduction of the knee extensor muscle activation of the AL with extension torque assistance in both incline and decline walking are similar to how previous hip and ankle exoskeletons were able to reduce the activation of the muscles that normally create the type of motion by providing torque at a given joint [5, 6, 26, 27]. Across the whole subject group in incline walking, the reduction of the knee extensor muscle activation is directly linked with the reduction of the total biological positive power generation of the knee joint on the AL. Even with the significant reduction of the knee extensor muscle activation, only about a half of the subject group were responders with assistance in both incline and decline walking. Therefore, the second hypothesis is rejected for both incline and decline walking is rejected.

Even though metabolic reduction was not consistently present across subjects, they consistently felt that they were using less effort with the assistance condition compared to the zero impedance condition for both incline and decline walking. Additionally, the

parameters for the commanded assistance torque profile were tuned based on the user's preference that were subjectively optimized for his/her own preferred gait. This result indicates that the user's metabolic cost was not always parallel with the subjects' subjective feeling on their level of effort. This result is also similar to other studies where the user's preference in two different types controllers and powered assistive timing did not correspond well with metabolic cost using a powered hip exoskeleton [27], [33]. Therefore, the negative result in the relationship between the user preference and metabolic cost additionally strengthens the argument that the tuning control parameter(s) based on the user's preference may not be optimal.

The difference in the responders' and nonresponders' metabolic responses with the assistance during incline walking can be explained by multiple aspects in the result in muscle activity and positive power generation. First, even though the reduction in muscle activation of the knee extensor group was commonly present in both responders and nonresponders in incline walking, the responders' reduction was higher in all knee extensor group of the AL than the nonresponders'. Also, the nonresponders' UAL traded the benefit of the torque assistance by increasing the activation of the knee extensors along with increasing the positive power generation of the knee joint. The responders did not demonstrate such compensatory behavior in terms of muscle activation and increase of positive power generation of the knee joint on the UAL. Importantly, the increase in total positive power generation as well as the increase of the total negative power absorption of both legs combined were observed from the incline nonresponders. This indicates that for the nonresponders during incline, the torque assistance was effective in partially replacing the muscle effort of the AL's knee extensor muscle group, but the user's gait in overall was

kinetically uneconomical during the assistance mode compared to zero impedance mode. On the other hand, in the incline assistance mode, the responders generally decreased the net positive power generation of all joints of both legs combined while maintaining the total negative power absorption from all joints on both legs combined unchanged from the zero impedance mode. Overall, the opposite trend in the change of total positive power generation and the activation level of the knee extensors on the UAL seemed the factors that differentiated the metabolic responses between the responders and nonresponders in incline walking.

The most distinctive difference in the muscle activation of the responders and nonresponders in decline walking was that the responders presented large reduction in the knee extensors muscle activation consistently in both AL and UAL whereas the nonresponders' were not as consistent as the responders. Both in incline and decline walking, the reduction in muscle activation of the knee extensors on both AL and UAL was the largest difference between the responders and nonresponders. Due to the limitation of the experiment, only two nonresponders' motion capture data were available for analysis, therefore, it may not be practical to conclusively explain the kinetic difference between the responders and nonresponders. However, the key factor to differentiate the kinetic behavior of the responders and nonresponders was the first 25% of the gait cycle. During the first 25% of the gait cycle in the zero impedance mode, the AL of the nonresponders was heavily relying on the ankle joint for the majority of the power absorption. On the other hand, during the first 25% gait cycle of the decline zero impedance mode, the responders were already utilizing the knee joint to cover about one third of the total power absorption of the leg. Based on this result, the nonresponders in decline may

not have needed extension torque assistance during the phase since the knee joint contribution was minimal as a shock absorber during the specific phase of gait cycle. It seems that the ankle joint may have been a better alternative compared to the knee joint to assist shock absorption for such nonresponders.

CHAPTER 7. CONCLUSION AND FUTURE WORK

Commonly in both incline and decline walking, the extension torque assistance during early stance phase was able to reduce the muscle activation of the AL. However, only about a half of the subject group have shown metabolic cost reduction with assistance in both incline and decline walking. The users also commonly preferred to walk with the assistance mode over the zero impedance mode in both incline and decline walking. Therefore, the user's subjective feeling on walking effort may not be an accurate factor in optimizing one's own metabolic cost. The opposite trend in total positive/negative power generation/absorption from both legs and increase of the muscle activation of the knee extensors on the UAL seemed to be what differentiated the responders and nonresponders in incline walking. In decline walking, whether the subject utilizes the knee joint as a shock absorber during weight acceptance may have differentiated the responders and nonresponders. For the use of a unilateral knee exoskeleton, the interaction between legs as well as the interaction between the device and the user should be considered to produce energetic benefit using a unilateral knee exoskeleton. One limitation of the study was that the device assisted only one leg. The biomechanical effects of bilateral knee exoskeleton in slope walking are sought to be investigated in the future. Also, experiments with different types of controller are also sought to be investigated since this study only tested one type of controller.

REFERENCES

[1] A. J. Young and D. P. Ferris, "State of the Art and Future Directions for Lower Limb Robotic Exoskeletons," *IEEE Transactions on Neural Systems and Rehabilitation Engineering,* vol. 25, no. 2, pp. 171-182, 2017.

[2] E. Guizzo and H. Goldstein, "The rise of the body bots [robotic exoskeletons]," *IEEE Spectrum,* vol. 42, no. 10, pp. 50-56, 2005.

[3] A. B. Zoss, H. Kazerooni, and A. Chu, "Biomechanical design of the Berkeley lower extremity exoskeleton (BLEEX)," *IEEE/ASME Transactions on Mechatronics,* vol. 11, no. 2, pp. 128-138, 2006.

[4] M. K. Shepherd and E. J. Rouse, "Design and Validation of a Torque-Controllable Knee Exoskeleton for Sit-to-Stand Assistance," (in English), *Ieee-Asme Transactions on Mechatronics,* vol. 22, no. 4, pp. 1695-1704, Aug 2017.

[5] G. S. Sawicki and D. P. Ferris, "Mechanics and energetics of incline walking with robotic ankle exoskeletons," (in English), *Journal of Experimental Biology,* vol. 212, no. 1, pp. 32-41, Jan 1 2009.

[6] T. Lenzi, M. C. Carrozza, and S. K. Agrawal, "Powered Hip Exoskeletons Can Reduce the User's Hip and Ankle Muscle Activations During Walking," (in English), *Ieee Transactions on Neural Systems and Rehabilitation Engineering,* vol. 21, no. 6, pp. 938-948, Nov 2013.

[7] G. Zeilig, H. Weingarden, M. Zwecker, I. Dudkiewicz, A. Bloch, and A. Esquenazi, "Safety and tolerance of the ReWalk™ exoskeleton suit for ambulation by people with complete spinal cord injury: A pilot study," *The Journal of Spinal Cord Medicine,* vol. 35, no. 2, pp. 101-96, 2012.

[8] A. Esquenazi, "New bipedal locomotion option for individuals with thoracic level motor complete spinal cord injury," *Journal of The Spinal Research Foundation,* vol. 8, no. 1, pp. 26-28, 2013.

[9] D. J. Farris and G. S. Sawicki, "The mechanics and energetics of human walking and running: a joint level perspective," *Journal of The Royal Society Interface,* p. rsif20110182, 2011.

[10] J. R. Montgomery and A. M. Grabowski, "The contributions of ankle, knee and hip joint work to individual leg work change during uphill and downhill walking over a range of speeds," (in English), *Royal Society Open Science,* vol. 5, no. 8, Aug 2018.

[11] A. S. McIntosh, K. T. Beatty, L. N. Dwan, and D. R. Vickers, "Gait dynamics on an inclined walkway," (in English), *Journal of Biomechanics,* vol. 39, no. 13, pp. 2491-2502, 2006.

[12] M. Kuster, S. Sakurai, and G. Wood, "Kinematic and kinetic comparison of downhill and level walking," *Clinical Biomechanics,* vol. 10, no. 2, pp. 79-84, 1995.

[13] A. N. Lay, C. J. Hass, and R. J. Gregor, "The effects of sloped surfaces on locomotion: Backward walking as a perturbation," (in English), *Journal of Biomechanics,* vol. 40, no. 13, pp. 3050-3055, 2007.

[14] N. Alexander and H. Schwameder, "Lower limb joint forces during walking on the level and slopes at different inclinations," (in English), *Gait & Posture,* vol. 45, pp. 137-142, Mar 2016.

[15] D. H. Wang, K. M. Lee, J. J. Guo, and C. J. Yang, "Adaptive Knee Joint Exoskeleton Based on Biological Geometries," (in English), *Ieee-Asme Transactions on Mechatronics,* vol. 19, no. 4, pp. 1268-1278, Aug 2014.

[16] J. H. Kim *et al.*, "Design of a Knee Exoskeleton Using Foot Pressure and Knee Torque Sensors," (in English), *International Journal of Advanced Robotic Systems,* vol. 12, Aug 20 2015.

[17] Y. Liao, Z. H. Zhou, and Q. N. Wang, "BioKEX: A Bionic Knee Exoskeleton with Proxy-Based Sliding Mode Control," (in English), *2015 Ieee International Conference on Industrial Technology (Icit),* pp. 125-130, 2015.

[18] B. Celebi, M. Yalcin, and V. Patoglu, "ASSISTON-KNEE: A Self-Aligning Knee Exoskeleton," (in English), *2013 Ieee/Rsj International Conference on Intelligent Robots and Systems (Iros),* pp. 996-1002, 2013.

[19] N. C. Karavas, N. G. Tsagarakis, and D. G. Caldwell, "Design, Modeling and Control of a Series Elastic Actuator for an Assistive Knee Exoskeleton," (in English), *2012 4th Ieee Ras & Embs International Conference on Biomedical Robotics and Biomechatronics (Biorob),* pp. 1813-1819, 2012.

[20] N. Karavas, A. Ajoudani, N. Tsagarakis, J. Saglia, A. Bicchi, and D. Caldwell, "Tele-Impedance based Stiffness and Motion Augmentation for a Knee Exoskeleton Device," (in English), *2013 Ieee International Conference on Robotics and Automation (Icra),* pp. 2194-2200, 2013.

[21] H. Zhu, J. Doan, C. Stence, G. Lv, T. Elery, and R. Gregg, "Design and Validation of a Torque Dense, Highly Backdrivable Powered Knee-Ankle Orthosis," *IEEE Int Conf Robot Autom,* vol. 2017, pp. 504-510, May-Jun 2017.

[22] K. Shamaei, P. C. Napolitano, and A. M. Dollar, "Design and functional evaluation of a quasi-passive compliant stance control knee-ankle-foot orthosis," *IEEE Trans Neural Syst Rehabil Eng,* vol. 22, no. 2, pp. 258-68, Mar 2014.

[23] K. Knaepen, P. Beyl, S. Duerinck, F. Hagman, D. Lefeber, and R. Meeusen, "Human-robot interaction: kinematics and muscle activity inside a powered

compliant knee exoskeleton," *IEEE Trans Neural Syst Rehabil Eng,* vol. 22, no. 6, pp. 1128-37, Nov 2014.

[24] G. Elliott, G. S. Sawicki, A. Marecki, and H. Herr, "The biomechanics and energetics of human running using an elastic knee exoskeleton," in *IEEE Conference on Rehabilitation Robotics*, 2013.

[25] G. Elliott, G. S. Sawicki, A. Marecki, and H. Herr, "The Biomechanics and Energetics of Human Running Using an Elastic Knee Exoskeleton," (in English), *2013 Ieee 13th International Conference on Rehabilitation Robotics (Icorr),* 2013.

[26] R. W. Jackson and S. H. Collins, "An experimental comparison of the relative benefits of work and torque assistance in ankle exoskeletons," *Journal of Applied Physiology,* vol. 119, no. 5, pp. 541-557, 2015.

[27] A. J. Young, H. Gannon, and D. P. Ferris, "A Biomechanical Comparison of Proportional Electromyography Control to Biological Torque Control Using a Powered Hip Exoskeleton," *Frontiers in Bioengineering and Biotechnology,* 10.3389/fbioe.2017.00037 vol. 5, p. 37, 2017.

[28] B. R. Umberger and P. E. Martin, "Mechanical power and efficiency of level walking with different stride rates," (in English), *Journal of Experimental Biology,* vol. 210, no. 18, pp. 3255-3265, Sep 15 2007.

[29] National Center for Health Statistics (U.S.) and National Health and Nutrition Examination Survey (U.S.), *Anthropometric reference data for children and adults : United States, 2011-2014* (Vital and health statistics Series 3, Data from the National Health and Nutrition Examination Survey, no. number 39). Hyattsville, Maryland: U.S. Department of Health and Human Services, Centers for Disease Control and Prevention, National Center for Health Statistics, 2016, p. p.

[30] J. Brockway, "Derivation of formulae used to calculate energy expenditure in man," *Human nutrition. Clinical nutrition,* vol. 41, no. 6, pp. 463-471, 1987.

[31] S. L. Delp, J. P. Loan, M. G. Hoy, F. E. Zajac, E. L. Topp, and J. M. Rosen, "An interactive graphics-based model of the lower extremity to study orthopaedic surgical procedures," *IEEE Transactions on Biomedical Engineering,* vol. 37, no. 8, pp. 757-67, 1990 1990.

[32] J. B. Dingwell, B. L. Davis, and D. M. Frazier, "Use of an instrumented treadmill for real-time gait symmetry evaluation and feedback in normal and trans-tibial amputee subjects," (in English), *Prosthetics and Orthotics International,* vol. 20, no. 2, pp. 101-110, Aug 1996.

[33] A. J. Young, J. Foss, H. Gannon, and D. P. Ferris, "Influence of Power Delivery Timing on the Energetics and Biomechanics of Humans Wearing a Hip Exoskeleton," *Front Bioeng Biotechnol,* vol. 5, p. 4, 2017.